LBL-37470
UC-410
Preprint

Lawrence Berkeley Laboratory

UNIVERSITY OF CALIFORNIA

Accelerator & Fusion Research Division

Submitted to Review of Scientific Instruments

Characterization of ALS Undulator Radiation—High K, Taper, and the Near Field Effect

D.A. Mossessian and P.A. Heimann

July 1995

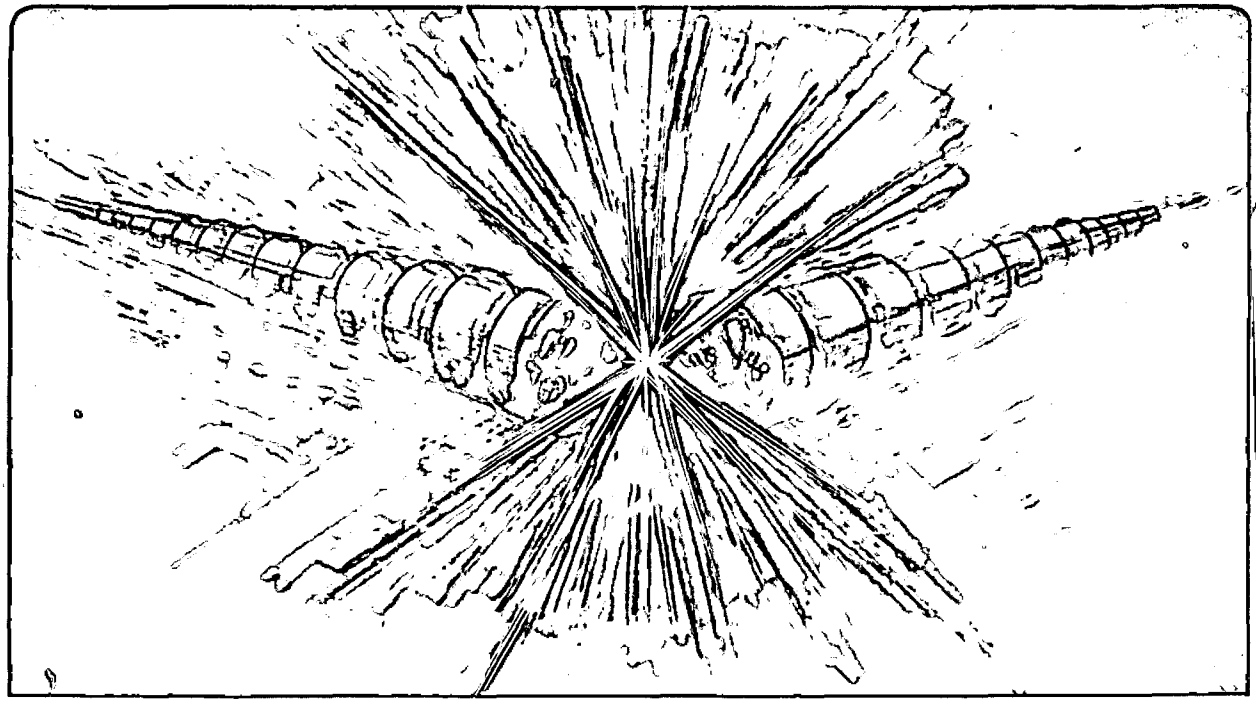

REFERENCE COPY
Does Not
Circulate
Bldg. 50 Library.
LBL-37470
Copy 1

Prepared for the U.S. Department of Energy under Contract Number DE-AC03-76SF00098

DISCLAIMER

This document was prepared as an account of work sponsored by the United States Government. While this document is believed to contain correct information, neither the United States Government nor any agency thereof, nor the Regents of the University of California, nor any of their employees, makes any warranty, express or implied, or assumes any legal responsibility for the accuracy, completeness, or usefulness of any information, apparatus, product, or process disclosed, or represents that its use would not infringe privately owned rights. Reference herein to any specific commercial product, process, or service by its trade name, trademark, manufacturer, or otherwise, does not necessarily constitute or imply its endorsement, recommendation, or favoring by the United States Government or any agency thereof, or the Regents of the University of California. The views and opinions of authors expressed herein do not necessarily state or reflect those of the United States Government or any agency thereof or the Regents of the University of California.

LBL-37470
LSBL-272
UC-410

CHARACTERIZATION OF ALS UNDULATOR RADIATION – HIGH K, TAPER, AND THE NEAR FIELD EFFECT*

D.A. Mossessian and P.A. Heimann

Advanced Light Source
Accelerator and Fusion Research Division
Lawrence Berkeley Laboratory
University of California
Berkeley, CA 94720, USA

Paper to be published by the Review of Scientific Instruments

*This work was supported by the Director, Office of Energy Research, Office of Basic Energy Sciences, Materials Sciences Division, of the U.S. Department of Energy, under Contract No. DE-AC03-76SF00098.

Light Source Note:
Author(s) Initials PJH 7/3/95 Date
Group Leader's initials HAP 7/3/95 Date

Characterization of ALS Undulator Radiation - high K, Taper, and the Near Field Effect.

D. A. Mossessian* and P. A. Heimann

Advanced Light Source, Accelerator and Fusion Research Division, Lawrence Berkeley Laboratory, Berkeley, California 94720

*Present address:

Synchrotron Radiation Center, University of Wisconsin-Madison, Stoughton, WI 53589

Abstract

The results of the measurements of spectral and angular distribution of the U5.0 (5 cm period) and U8.0 (8 cm period) Advanced Light Source undulators are described. The spectra of on-axis undulator radiation were measured for various values of the deflection parameter K. In particular, the high K case was studied, representing the region between the undulator and wiggler limits. Good agreement in harmonic peak flux and width is found between the measurements and the computations that include the real magnetic field, the electron beam energy spread and the electron beam emittance. The effect of the undulator taper on the spectral characteristics of the radiation was analyzed. At small taper (~ 0.5% gap variation) significant reduction in peak brightness and flux of the fifth harmonic was observed with small effect on the fundamental. The near field effect in the undulator radiation was studied by measuring the off-axis spectral and angular distributions of the radiation. The broadening and the fine structure in the distributions at large off-axis angles was observed, resulting from the near field effect.

Introduction

In the early operation of the Advanced Light Source (ALS) three undulators - two U5.0 (5 cm period, 89 periods) and one U8.0 (8 cm period, 55 periods) - were installed in the storage ring. Prior to the commissioning of the undulator beamlines the radiation from both U5.0 and U8.0 undulators was characterized. The goals of the measurements were to verify the performance of the ALS undulators, to test the accuracy of the undulator radiation calculations, and to examine special characteristics of undulator radiation such as taper and near field effect.

The first results of the measurements of the U5.0 undulator were reported in a short communication [1], which contained on-axis spectra at two K values, 0.44 and 2.12, and angular distributions near the undulator axis. In this paper we present the results of the U8.0 measurements and additional U5.0 results. The on-axis undulator spectra were recorded and the spectral width and absolute flux per unit solid angle of the harmonics were derived. The undulator deflection parameter K was varied over a wide range (from 0.44 to 5.24) that includes the transition between undulator and wiggler limits. A comparison has been made between undulator radiation calculations and the measurements. The calculations have been performed using URGENT [2] and UR [3] computer codes. The codes employ different approaches to the undulator radiation computations. The URGENT code uses the Bessel function approximation starting with an ideal magnetic field. The effect of emittance is taken into account by convoluting the single electron spectrum with the electron beam phase space area. The UR code can use either ideal or measured magnetic field of an undulator and calculates radiation of a relativistic electron passing through the device from general radiation formulae. The Monte-Carlo method is then used to simulate the electron beam emittance. Comparison with calculations makes it possible to analyze individually the effects of the electron beam emittance, energy spread and magnetic field.

One of the undulator parameters that can alter the characteristics of the radiation is taper. The introduction of taper in an undulator leads to reduction of the peak brightness and spectral

broadening of each harmonic. For the U5.0 undulator, harmonics at different small values of undulator taper were recorded, and changes in the spectral width and absolute brightness were observed. The initial goal of these measurements was to verify the alignment of the undulator magnetic structure. Also, the effect of tapering on the fundamental and fifth harmonic was analyzed.

Besides the measurements of the on-axis undulator radiation, which are essential for the evaluation of the undulator beamlines, the angular and spectral characteristics of the off-axis radiation were also studied. Particular attention was paid to the near field effect that influence the properties of this radiation. The results of these measurements were compared with the theory for the near field effect, developed by R. Walker for the single electron case [4]. In addition, the effect of the emittance on the off-axis radiation was studied.

The measurements were performed with the Transmission Grating Spectrometer (TGS) that was designed specifically for undulator radiation characterization. A detailed description of the design and calibration of the spectrometer and of the experimental setup has been presented previously [5]. The TGS consists of a spherical focusing mirror, two interchangeable gold transmission gratings, and a Si n on p photodiode behind a 10 μm slit. The resolving power of the spectrometer, $\lambda/\Delta\lambda$, was measured to be around 200 for the first order of diffraction and 630 for the fourth order. During the measurements the TGS was installed after the beamline front end at a distance of 15.5 m from the center of the undulator. The angular resolution of the TGS was determined by the size of two interchangeable pinholes in front of the grating, which set the angular acceptance from the source to 20 μrad or 10 μrad. The measurements were performed in two ways. Undulator radiation spectra were recorded by scanning the detector for a fixed position of the spectrometer with respect to the photon beam. Angular distributions of radiation were obtained by translating the spectrometer as a whole with constant TGS photon energy setting (fixed detector position in the diffraction plane of the grating). For an angular scan in the vertical direction, the position of the detector was corrected for the change in the incidence angle on the grating. In order to protect the gratings from damage, the radiation power density on the gratings

was limited to 0.1 W/cm^2 during the undulator radiation measurements. This power restriction translated into a storage ring current between 0.1 and 1 mA depending on the undulator gap.

On axis undulator radiation spectra - theory and measurements.

The spectra of on-axis undulator radiation were observed for different undulator gaps, for which the undulators' magnetic field was previously mapped [6]. For the U8.0 undulator five K values were studied, K = 0.44, 0.9, 1.79, 2.82, and 5.24. Here we discuss the U8.0 on-axis measurements, whose range of K values exceeded the U5.0 experiment. The same effects, the electron beam emittance and energy spread and the non-ideality of the magnetic field, influence the on-axis spectra of both U8.0 and U5.0 undulators. The strength of these effects is evaluated by comparing the measured harmonics of the U8.0 radiation with computations.

The properties of the measured harmonics are very sensitive to the position of the TGS relative to the axis of the radiation central cone. To determine the on-axis position of the spectrometer for each gap the angular distribution of the 5th harmonic central cone was recorded in both vertical and horizontal planes. The measured spectra were normalized to the current of the electron beam that was recorded during the scan together with the signal from the detector. The absolute flux of the harmonics was obtained from the recorded data using the measured efficiencies of the TGS optical elements. In the recorded spectra each harmonic contains contributions from the higher orders of diffraction of the higher harmonics. To determine the peak brightness of individual harmonic these contributions were accounted for using the measured efficiencies of the transmission grating [5]. Estimations show that the angular acceptance of the spectrometer is always smaller than the angular width of the central cone combined with the angular divergence of the electron beam. Thus, the on-axis flux per unit solid angle of the harmonics can be calculated by dividing the measured flux by the angular area of the spectrometer aperture.

The resolving power of the TGS in the first order of diffraction of the transmission grating is comparable to the widths of the higher harmonics in the spectra. Therefore, the shape and

intensity of the higher harmonics in the spectrum are also affected by the spectrometer instrument function. To analyze individual harmonics the fourth order of diffraction of the transmission grating was used, having the resolution smaller than the harmonic widths. To obtain the peak flux, the integrated power of a harmonic, measured in the fourth order of diffraction, was normalized to be equal to the power in the first order. This method takes advantage of the more accurate calibration of the first order of diffraction and the better resolution of the higher orders.

Fig. 1 shows spectra of the U8.0 undulator for 85 mm, 39 mm, and 25 mm gaps, corresponding to the deflection parameter K values 0.44, 2.82, and 5.24 respectively. In the spectrum at K = 5.24 the fundamental and the harmonics between 9 and 18 were not recorded. Also, the spectra shown in this figure have not been corrected for the higher orders of diffraction.

The figure illustrates the change of the spectral characteristics of the radiation as the operational mode of the insertion device changes from the undulator limit ($K \leq 1$) to the wiggler limit ($K >> 1$). With K value increasing, the number of the harmonics in the spectrum increases and the power of the higher harmonics becomes higher than the power in the fundamental. More then 90 harmonics can be seen in the K=5.24 spectrum, while the K=0.44 spectrum shows only three harmonics.

The complexity of the spectrum at K=5.24 makes it difficult to quantitatively analyze the contribution of the higher orders of diffraction and of the background below the individual harmonics. The spectral shape and intensity of the low harmonics were analyzed for lower K values. Particular attention was paid to the first, third and fifth harmonics that are used in the ALS undulator beamlines. It was found that, as the harmonic number n increases, the width of the harmonics $\Delta E/E$ approaches a constant limit rather than decreasing as $1/nN$, N being the number of periods in the insertion device. The measured, calculated and ideal width of the first 9 harmonics at K=2.82 (39 mm gap) is shown in Fig.2. The calculations of the harmonic widths were performed using the URGENT code, which includes the effect of the electron beam emittance. The electron beam energy spread was taken into account by convoluting the URGENT spectra with a

Gaussian function whose width $\Delta E/E$ was calculated using the theoretical value of $6.5 \bullet 10^{-4}$ for the rms relative energy spread. The results of the measurements and calculations agree well. The finite width of the TGS instrument function, that was not taken into account during the analysis of the measured spectra, may explain the small differences between calculated and measured widths. Calculations performed using the UR code, that includes the real undulator magnetic field, show no discernible effect of the real field on the widths of the harmonics presented in Fig.2.

The deviation from the ideal width observed in Fig.2 is produced by the effects of the electron beam emittance and energy spread. These effects can be estimated using the general formula for the harmonic wavelength

$$\lambda_n = \frac{\lambda_u}{2n\gamma^2}\left(1+\frac{K^2}{2}+\gamma^2\theta^2\right) \qquad (1)$$

where n is the harmonic number, λ_u is the undulator period, K is the deflection parameter and θ is the observation angle. Following this formula, the change of the observation angle from zero to θ leads to the change of the harmonic energy ΔE. Then, the effect of the emittance on the harmonic width may be estimated by taking into account the spread of observation angle due to the finite size and divergence of the electron beam σ_e:

$$\frac{\Delta E_e}{E} = \frac{\gamma^2\sigma_e^2}{\left(1+K^2\right)} \qquad (2)$$

The electron beam energy spread $\Delta\gamma/\gamma$ leads to the harmonic broadening as

$$\frac{\Delta E_{es}}{E} = 2\frac{\Delta\gamma}{\gamma} \qquad (3)$$

Following Eqs. (2) and (3) both energy spread and emittance have contributions to $\Delta E/E$ independent of harmonic number. The contribution of the energy spread is constant for all undulator gaps, while the effect of the emittance depends on K value. For the ALS electron beam,

the harmonic widths are affected mainly by emittance for $K \leq 2$, but determined mostly by the energy spread for larger K values. For the lower harmonics the effects of emittance and energy spread combine with the intrinsic width (1/nN). As harmonic number n increases, the width approaches an asymptotic value determined by the emittance and energy spread alone. An asymptotic value of ~ 1/250 is calculated for K=2.82 from the known emittance and energy spread. This estimated result is consistent with the measured odd harmonics shown in Fig.2. However, it is seen from the Fig.2 that the widths of the even harmonics is generally larger than those of the odd harmonics. This difference can be explained by the fact that the even harmonics have no intensity on axis in the single electron approximation. As a result, their spectral width is affected to a greater extent by the phase space distribution of the electron beam.

The measured individual harmonics were compared with the results of calculations performed with the UR and URGENT codes. The detailed comparison of the U5.0 radiation measurements with the results of calculations performed using URGENT was made in [1]. It was found, that the measured harmonics' shape and width are well reproduced in the calculations. The measured harmonics' peak brightness was systematically higher than the calculated one by 20 - 25%. This difference was caused by an error in the electron beam current measurements and by an uncertainty in the spectrometer calibration. During the period between the U5.0 and U8.0 experiments the storage ring current measurement was improved allowing a tolerance of 1% for the current normalization in the present work. Better agreement was therefore found between the results of U8.0 measurements and URGENT and UR calculations.

Fig.3 shows the measured and calculated (UR) harmonics of the U8.0 undulator at K of 0.44, 0.9, and 1.79. In agreement with the previous results, the measured width and shape of the harmonics are well reproduced by the calculations in all cases. In general, the difference in peak flux per unit solid angle between measurements and calculations does not exceed 15%. The only case of significant disagreement is found for the fundamental at K=1.79, where the computed brightness is about 35% lower than the measured one. However, the contribution of the higher orders of diffraction to this peak is quite large (about 50%). Thus, the error may be caused by the

uncertainty in the measured efficiencies of the higher orders of diffraction of the transmission grating.

Comparison of the results of URGENT and UR computations showed that in most cases the difference in the spectrum from the real or ideal magnetic field is small. However, for the peak intensity of the third and fifth harmonics at K=0.44, significant disagreement was found between the measurement and the calculation with URGENT. In the case of the fifth harmonic the measured peak flux density is about 50% of the URGENT calculated flux. The UR code gave better agreement with the measurement, suggesting that magnetic field errors have significant influence at the lowest K. This conclusion is consistent with the magnetic field measurements [6], which determined a larger rms field error at this gap ($\sigma \approx 0.06\%$) than at smaller gaps ($\sigma \approx 0.025\%$ - 0.035%).

The measurements of the on-axis flux per unit solid angle of the undulator radiation can be used to analyze the effect of the electron beam emittance, energy spread, and field errors on the brightness and flux of the harmonics. The emittance increases the photon beam phase space area. As a consequence, while the brightness of the undulator source is decreased by the emittance, the flux of a harmonic integrated over the central cone remains constant. The electron beam energy spread does not affect the angular characteristics of the radiation since the dispersion in the ALS straight sections is zero. Therefore, the energy spread is an especially critical parameter since it affects both brightness and flux. The magnetic field errors can also affect both brightness and flux, but their effect on the lower harmonics is in general very small for the ALS undulators. These conclusions are confirmed by the agreement between the measured harmonics angular distributions and calculations including only the electron beam emittance.

For high harmonics, however, the effect of magnetic field errors can be quite significant. The influence of the real magnetic field together with emittance and energy spread was analyzed in the spectrum at K=5.24. In Fig.4 are displayed the high harmonics (n >18) at K=5.24 calculated with the ideal field, the real field calculations, and the measured spectrum. All calculations include electron beam emittance and energy spread and are convoluted with the TGS instrument function.

As it was mentioned above, the width and, consequently, the peak flux of the high harmonics in the ideal field case is determined mostly by the energy spread.

The individual harmonics in the measured spectrum continue to be resolved up to 90th harmonic. This observation suggests that the insertion device still works as an undulator, with the radiation spectrum resulting from an interference of waves, emitted by the electron from each magnetic period. For an undulator with an ideal magnetic field, the on axis flux per unit solid angle is larger than that of a bending magnet by about a factor of N^2. If the interference is not present, the spectral distribution of radiation would be represented by a smooth curve and the bending magnet approximation would be valid. This wiggler radiation spectrum can be calculated simply by multiplying the bending magnet spectrum by 2N. In Fig.4 the wiggler approximation curve is shown calculated for the magnetic field B=0.7 T (peak value for U8.0 undulator at K=5.24). For this value of B the critical energy is $E_c = 1068$ eV. It is seen, that the peak flux per unit solid angle of the harmonics decreases with increasing energy, approaching the wiggler curve above critical energy.

The overall agreement between the measurement and the real field calculation is good. Around the critical energy the harmonics begin to partly overlap, producing a radiation continuum that is observed in the measured spectrum. The difference in the harmonic height between measurement and calculation is caused by the contribution of the background and the higher orders of diffraction. The overall shape of the measured spectrum is also affected by the shape of the background that was approximated by a straight line and then subtracted from the measured data. The effect of the magnetic field errors is clearly seen. The peak flux of the twentieth harmonic is about 50% lower then the calculation with ideal field. As the harmonic energy increases, the errors in the magnetic field have an increasing influence on flux. In the high harmonics limit ($n > 50$) the spectrum of the radiation emitted from the real undulator approaches that of a wiggler.

When comparing the results of the measurements and calculations experimental errors should be taken into account as well as assumptions used in the calculations. The error in the spectrometer efficiency and the error in the electron beam current were mentioned above. The least

understood source of the error is the background in the spectra, which consists of scattered visible, UV, and soft x-ray radiation. During the analysis this background was approximated by a line joining the minima between harmonics. In the calculations, the measured value of the electron beam emittance [1] and the theoretical value of the energy spread were used. Uncertainty in the values of the emittance and the energy spread may lead to discrepancies between the measurements and calculations.

Spectra of tapered undulator

The spectral characteristics of the on-axis radiation can be changed if taper is introduced to the undulator. Taper leads to a variation of the peak magnetic field and of the deflection parameter K along the device, thus changing the width of the radiation harmonics. One of the motivations for studying tapered undulators is the possibility to obtain a broadened harmonic, producing a wide spectral range source without the necessity of tuning the undulator gap. The spectral characteristics of the radiation from a tapered undulator were examined experimentally in [7] for an undulator at a high energy storage ring producing hard x-rays.

Measurements of the U5.0 undulator spectra were done for a series of tapers with the variation of the gap Δg between the two ends of the undulator changing by about 30 μm between measurements. The average gap was fixed at a value of approximately 23 mm, giving K of 2.12. One of the goals was to verify that the initial alignment of the undulator was without taper. It was found that the initial alignment of the device was optimum for obtaining the narrowest harmonics.

A simple model was used in [7] to estimate the effect of the taper on the undulator radiation spectrum. Taking into account the relationships between the undulator deflection parameter K and the undulator gap g, the change in the harmonic width due to the taper Δg was estimated

$$\frac{\Delta E}{E} \approx \frac{K^2}{1+K^2/2}\frac{\pi \Delta g}{\lambda_u} \qquad (4)$$

If the harmonic FWHM of a non-tapered undulator is ΔE_0, the width of the harmonic from the tapered device is approximately

$$\Delta E_{total} \approx \sqrt{(\Delta E_0)^2 + (\Delta E)^2} \qquad (5)$$

where ΔE is given by Eq.(4). The width of the harmonics due to taper remains constant for a given value of Δg, while the natural width of the harmonics decreases with increasing n. Therefore the higher harmonics will be more affected by the taper than the fundamental.

The first and fifth harmonics measured at different tapers are shown in Fig.5. It is seen, that while the width of the fundamental changes little with the taper varying from 0 to 125 μm, the fifth harmonic is broadened by almost a factor of 3 at the maximum taper. Calculations using UR, performed in the single electron approximation, show that the fifth harmonic at 125 μm taper is split into two peaks. In the measured spectrum these peaks are smoothed out by the effect of the emittance. The calculated widths of the harmonics, estimated using Eqs.(4,5) are listed in Table 1 and are in good agreement with the observed values.

Analysis of the angular distribution of the central cone shows that the effect of the taper on the phase space of the radiation is significant. The observed relative increase in the vertical angular width is greater than in the horizontal because of the smaller vertical emittance of the electron beam. For the fifth harmonic, the measured angular width increases from about $7 \bullet 10^{-3}$ mrad^2 to about $11 \bullet 10^{-3}$ mrad^2 at 0 and 125 μm taper respectively. As a consequence of the broadening of the angular distribution, taper reduces both the flux per unit solid angle (photons/sec/0.1%BW/mrad^2) and the flux integrated over the central cone (photons/sec/0.1%BW). But the flux per unit solid angle decreases more, a factor of 2.3, in comparison with the integrated flux, which is reduced by about 30 %.

Although the effect of taper on the angle-integrated harmonic flux is not as large as on the harmonic brightness, it can be important at large tapers. Therefore ,at a storage ring such as the

ALS, to preserve undulator performance in terms of brightness as well as flux, tuning the undulator gap may be more suitable than using taper to obtain a wide spectral range. However, since the higher harmonics are more affected by taper than the fundamental, it may be possible to use the reduction in flux of the higher harmonics in order to suppress higher orders of diffraction. This technique would be most suited to monochromators that use the first harmonic.

Near field effect in the off-axis undulator radiation.

In both the URGENT and UR computer codes the far field approximation is used, which is correct when the distance between the source and the observer is large compared to the undulator length. However, as it was shown in [4], the near field effects can be important when the radiation is observed off the undulator axis. In practice, this effect leads to broadening of the harmonics depending on the off-axis angle θ. At large angles a splitting of the harmonics into two or more peaks was predicted.

When the radiation is viewed off-axis at an angle θ and the distance between the center of the undulator and the observation point D is assumed infinite, the wavelength of the nth harmonic of the radiation is determined by the Eq.(1). For this wavelength the path difference for the radiation emitted from the center and the ends of the undulator is equal to the integral numbers of λ. This is also true when the distance D is finite but the radiation is observed on-axis. At an off-axis angle θ, when the distance D is finite, there is an additional path difference for the waves emitted from the center and the ends of the device. This path difference is given in a first approximation as $L^2\theta^2/8D$. The parameter

$$W_n = \frac{nL^2\theta^2}{2\lambda_1 D} \qquad (6)$$

was introduced in [4] as a measure of the corresponding phase difference for the nth undulator harmonic. When W = 1, there is a $\pi/2$ phase difference between an end and the center of the undulator. $W \geq 1$ may be taken as a condition for observing near field effects.

The spectral linewidth from the near field effect may be estimated by converting the change in observation angle as a wavelength change using Eq.(1). Then the harmonic full width at half maximum is approximated by

$$\Delta\lambda \approx \frac{1}{2}\frac{\lambda_u}{2n}\left(\theta_1^2 - \theta_2^2\right) \approx \frac{1}{2}\frac{\lambda_u}{n}\frac{L\theta^2}{D} = \frac{W_n}{nN}\lambda_n \qquad (7)$$

where θ_1 and θ_2 are the observation angles at the ends of the insertion device.

Analysis of the radiation from an ideal undulator in the single electron approximation was performed in [4] to determine the reduction in the harmonic intensity and the broadening of the lineshape. It was shown, that as the parameter W increases, the harmonic splits into two or more peaks, the number of peaks being equal to W/2. Results of numerical calculations showed that the reduction in harmonic peak intensity is oscillating around the value of 2W. In practice the electron beam in the storage ring has a finite emittance, which leads to a broadening of the harmonics. If an electron trajectory has an angle $\Delta\theta$ to the undulator axis, the observation off-axis angle becomes $\theta \pm \Delta\theta$. Thus, the effect of the electron beam emittance can be estimated using Eq.(7) with θ_1 and θ_2 substituted by $(\theta + \sigma_e)$ and $(\theta - \sigma_e)$, where σ_e is the rms size of the angular distribution of the electron beam in the plane of the undulator axis and the direction of observation. The contribution of the emittance perpendicular to the observation plane is small because the observation angles θ are in general much greater than σ_e The value σ_e includes both the rms size σ and angular divergence σ' of the electron beam, according to $\sigma_e = \sqrt{(\sigma')^2 + \sigma^2/D^2}$. The broadening of the harmonic due to the electron beam emittance is then given by

$$\Delta\lambda = \frac{\lambda_u}{2n}\left[(\theta+\sigma_e)^2 - (\theta-\sigma_e)^2\right] = 2\frac{\lambda_u}{n}\theta\sigma_e \qquad (8)$$

It is seen from the Eq.(7) and Eq.(8), that the near field effect varies with θ^2, while the effect of the emittance depends on θ linearly. Therefore, there will be a range of small angles for which the emittance effect is more important. Comparison of the Eqs.(7) and (8) shows that the near field effect becomes larger than the broadening from emittance when the off-axis observation angle

$$\theta \geq \frac{4\sigma_e D}{L} \equiv \theta_0$$

In contrast to W, θ_0 does not have a dependence on harmonic number n.

The near field effect was studied in spectra of the U8.0 undulator at 67 mm gap, corresponding to the K value of 0.9. The angular divergence of the electron beam in horizontal direction was measured previously and is σ_e = 25 μrad. For this value of σ_e, the angle θ_0, for which the near field effect should start exceeding the effect of the emittance, is ~ 350 μrad ($W_1 \approx$ 8). In vertical direction the beam divergence is smaller (σ_e = 9 μrad) leading to a smaller value of $\theta_0 \approx$ 130 μrad ($W_1 \approx 2$). Measurements were performed for four off-axis angles - 90, 140, 190, and 380 μrad, corresponding to values of W_1 of 1, 2, 4, and 8. A spectrum corresponding to W_1=8 in the horizontal direction could not be recorded because of low intensity of the radiation. At each angle, the angular distribution of the fundamental was measured as well as the energy spectrum.

The off-axis angular distributions of the fundamental are shown in Fig.6. These distributions were obtained by shifting the TGS detector by 9.4, 21.2, and 35.7 eV below the fundamental energy on axis, which corresponds to W_1 of 1,2, and 4. In the horizontal direction the angular FWHM of the distribution is close to the angular width from emittance $2.35\sigma_e$ and increases only slightly due to the near field effect with the increasing off-axis angle θ. This result is

consistent with the estimations described above. The measured peak intensities and angular profiles are both in good agreement with calculations using URGENT. This agreement with the far field calculations shows that the properties of the undulator radiation at these horizontal angles are still mostly determined by the beam emittance. For the off-axis angular distribution in the vertical direction where the emittance is smaller, the angular width is observed to increase dramatically with angle θ. There is agreement between the measurements and far field calculations only in the case of $W \leq 2$ for the distributions measured above the undulator axis. Below the undulator axis the angular profile is broadened more than calculation for all three W_1 values and a splitting of the fundamental is observed for $W_1 = 4$. Thus, the near field effect is seen to have a stronger influence on the angular distribution in the vertical plane than in the horizontal plane.

The near field effect can be seen in further detail in undulator radiation spectra observed at vertical off-axis angles. Fig.7 displays vertical off-axis spectra for the angles 190 and 380 μrad, corresponding to $W_1 = 4$ and 8. Splitting of harmonic peaks is again seen. For the spectra below the undulator axis the fundamental splits into $W_1/2$ peaks. In each off-axis spectrum all harmonics show a remarkably similar profile, both in terms of the number of peaks and the linewidth $\Delta E/E$. This result is consistent with Eqs. (7) and (8) predicting the same dependence on harmonic number n for the near field effect and for emittance. An unexpected difference is observed between the spectra measured above and below the undulator axis. This asymmetry could be caused by a horizontal dipole field B_x, which results in an electron trajectory having a vertical angle varying along the length of the undulator.

The calculation of the near field effect by R. Walker [4] considers only the single electron case and, therefore, direct comparison with the measurements is not possible. However, features predicted in [4] should be seen in measured spectra, where the near field effect dominates the emittance effect. Such is the case for the spectrum observed at the off-axis angle of 380 μrad (W_1=8) below the undulator axis. The fundamental in the spectrum is split into four ($W_1/2$) peaks. The width of the harmonics in this spectrum agrees well with results of a calculation performed

using the analytical model developed in [4]. The predicted asymmetry of the harmonics lineshape where the higher energy peak in the harmonic structure is larger than the lower energy one can also be found in the measured harmonics in the vertical plane. Further measurements as well as calculations including both the near field effect and emittance would be valuable.

Conclusion.

Properties of undulator radiation on and off the insertion device axis were studied. Measured on-axis undulator radiation spectra demonstrated good performance of the ALS undulators. The spectral shape and flux of the harmonics are determined mainly by the intrinsic lineshape and by the electron beam properties (emittance and energy spread). In most cases, the effect of the real undulator magnetic field compared to the ideal field is small. In particular, the high quality of the magnetic field is seen in case of high K spectra, where more than 90 harmonics are observed and the peak flux per unit solid angle of the twentieth harmonic reduced only by 50% compared with the ideal field case.

Analysis of the radiation from the tapered undulator shows that while taper increases the linewidth of the harmonics, the brightness and even the flux of the harmonics are also significantly reduced. On the other hand, the larger effect of the taper on the higher harmonics compared with the fundamental makes it a possible technique for suppressing the higher harmonics in undulator spectra.

When measuring the off-axis undulator radiation spectra, a change in the spectral characteristics of the radiation was recorded, resulting from the near field effect. The near field effect and electron beam emittance have competing influence on the harmonics. The observed features: the broadening and splitting of the harmonics, and the asymmetry of the harmonics' lineshape, are qualitatively consistent with the theoretical predictions.

Acknowledgment

The authors would like to thank R.P.Walker (ELETTRA) for making the URGENT program available and R.Dejus (APS) for making the UR program available. The authors are grateful to R. Klein (BESSY) for performing additional calculations of the undulator radiation. H.Padmore is thanked for helpful discussions.

This work is supported by Director, Office of Energy Research, Office of Basic Energy Sciences, Materials Sciences Division of the US Department of Energy under Contract Number DE-AC03-76SF00098.

Figure captions:

1. U8.0 spectra for different K values. The measured flux per unit solid angle is normalized to 400 mA electron beam current.

2. Measured and calculated widths of the first nine harmonics in the U8.0 spectrum at K=2.82.

3. Measured (solid line) and calculated (dotted line) first, third and fifth harmonics at different K values. Calculations with UR include the electron beam emittance, energy spread, and the real undulator magnetic field.

4. High harmonics at K=5.24. (a) - ideal field calculation. (b) - measurement (dotted line) and real field calculation (solid line). In (b) the bending magnet approximation multiplied by 2N is also shown (dashed line).

5. Measured first (a) and fifth (b) harmonics of U5.0 radiation for different undulator tapers at average gap of 23 mm (K=2.12).

6. Measured (solid lines) and URGENT calculated (dotted lines) angular distributions of the red shifted fundamental corresponding to values of W_1 of 1, 2, and 4. Top - angular distribution in the horizontal plane, bottom - angular distribution in the vertical plane.

7. Vertical off-axis spectra measured below and above the undulator axis. The inserts display the higher harmonics with an expanded vertical scale.

Table 1: Measured and calculated width of first and fifth U5.0 harmonics for different undulator taper.

References:

1. P.A.Heimann, D.A.Mossessian, A.Warwick, C.Wang, S.Marks, H.Padmore, B.Kincaid. Rev. Sci. Instrum. **66** (2), 1885 (1995

2. R. Walker, B. Diviacco. Rev. Sci. Instrum **63** (1), 392 (1992)

3. Roger J. Dejus, Alfredo Luccio. Nucl. Instrum. Methods A **347**, 61 (1994)

4. R.Walker. Nucl. Instrum. Methods A **267,** 537 (1988)

5. D.A.Mossessian, P.A.Heimann, E,Gullikson, R.K.Kaza, J.Chin, J.Akre. Nucl. Instrum. Methods A **347,** 244 (1994)

6. S. Marks, D. Humphries, B. Kincaid, R. Schlueter, and C. Wang. Proc. SPIE **2013**, 171 (1993)

7. B.Lai, P.J.Viccaro, R.J.Dejus, E.Gluskin, W.B.Yun, I.McNulty, Rev. Sci. Instrum. **64** (4), 858 (1993)

D A Mossessian
P.A. Heimann

Table 1

Δg (μm)	$\Delta\lambda_{1meas}$ (Å)	$\Delta\lambda_{1calc}$ (Å)	$\Delta\lambda_{5meas}$ (Å)	$\Delta\lambda_{5calc}$ (Å)
0	1	1	0.088	0.09
90	1.1	1.23	0.15	0.16
125	1.2	1.4	0.22	0.22

D A. Mossessian
P.A. Heinmann

Figure 1.

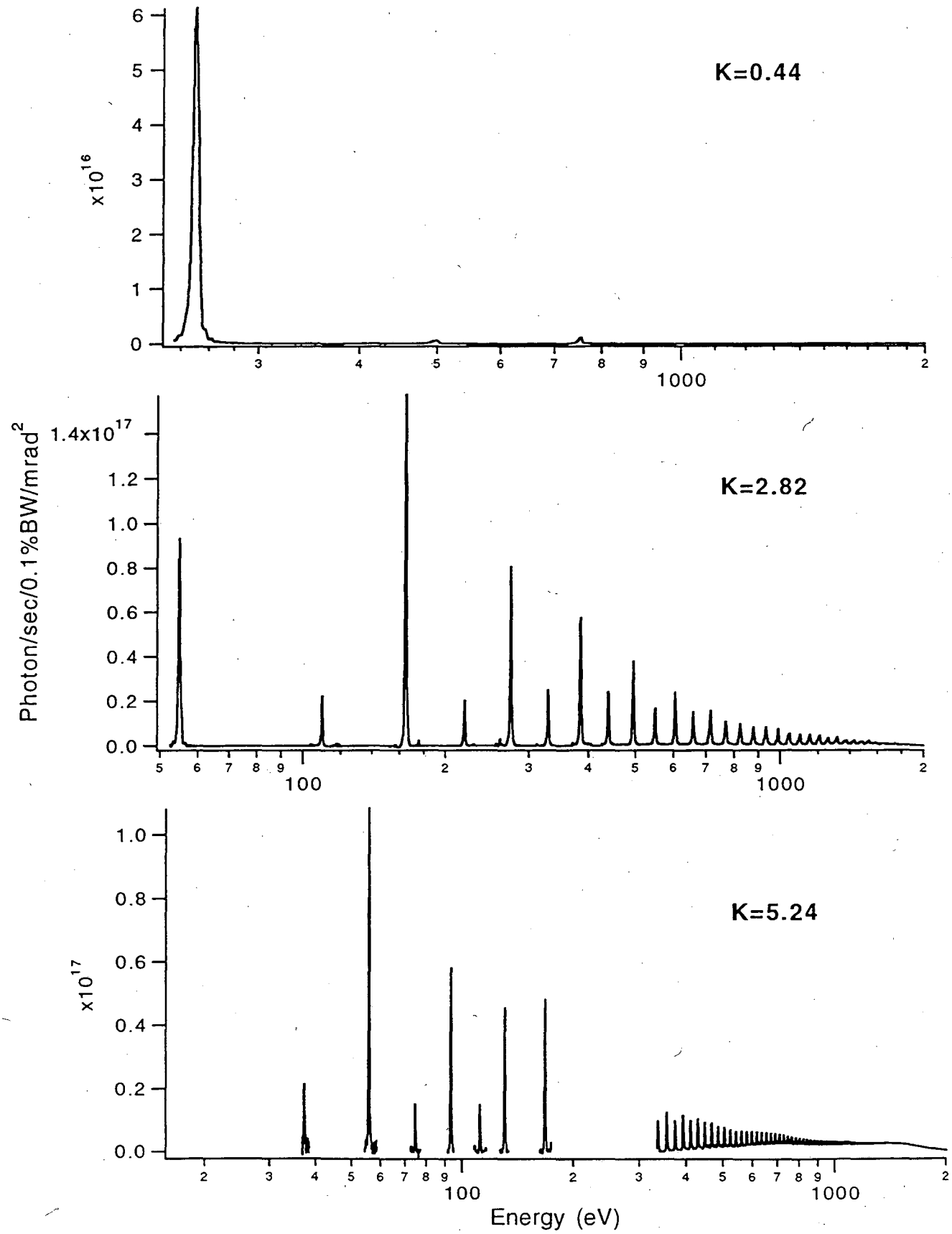

D.A Mossessian
P.A Fleinman

Figure 2.

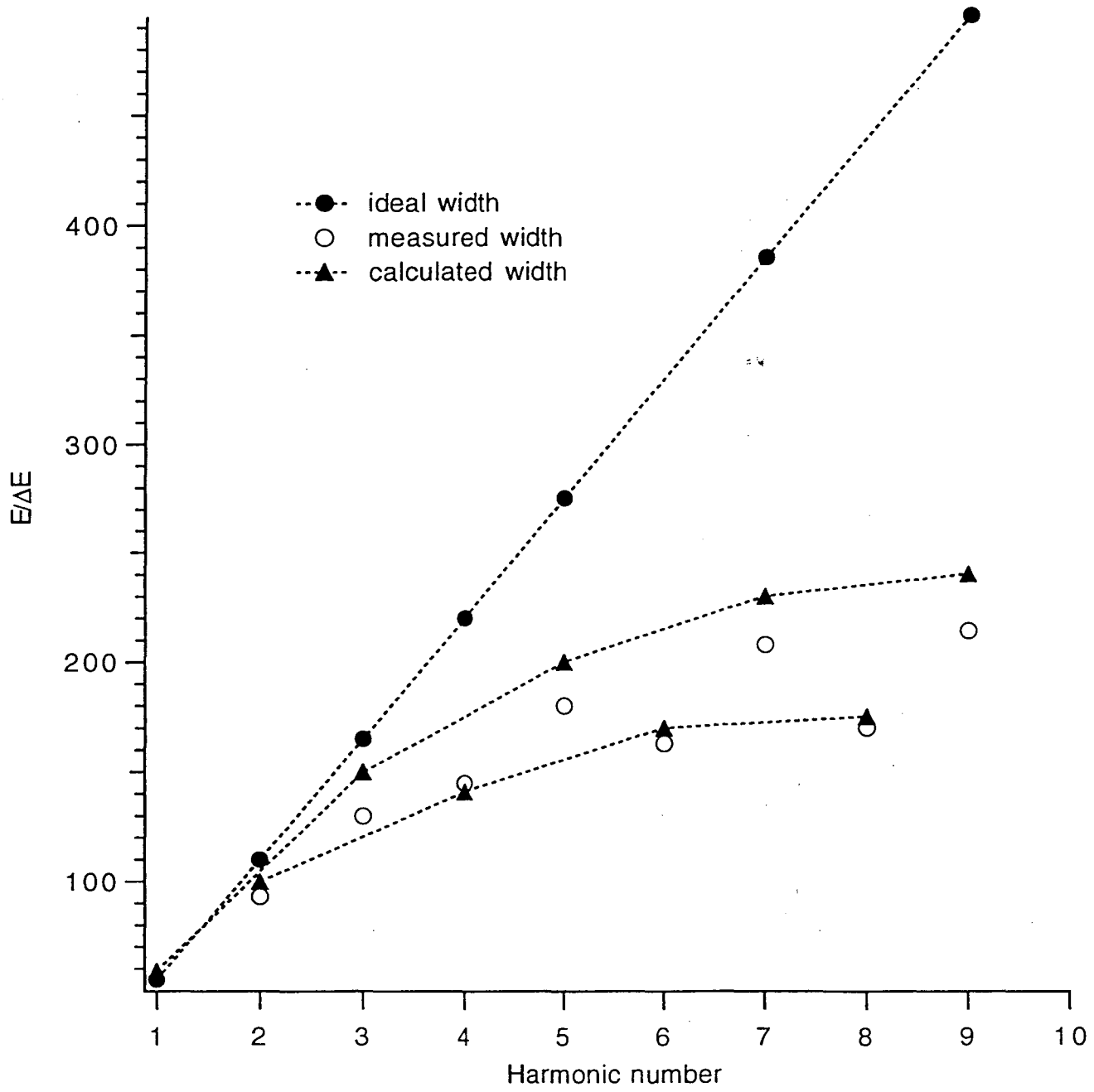

D A Mossessian
D.A. Heimann

Figure 3

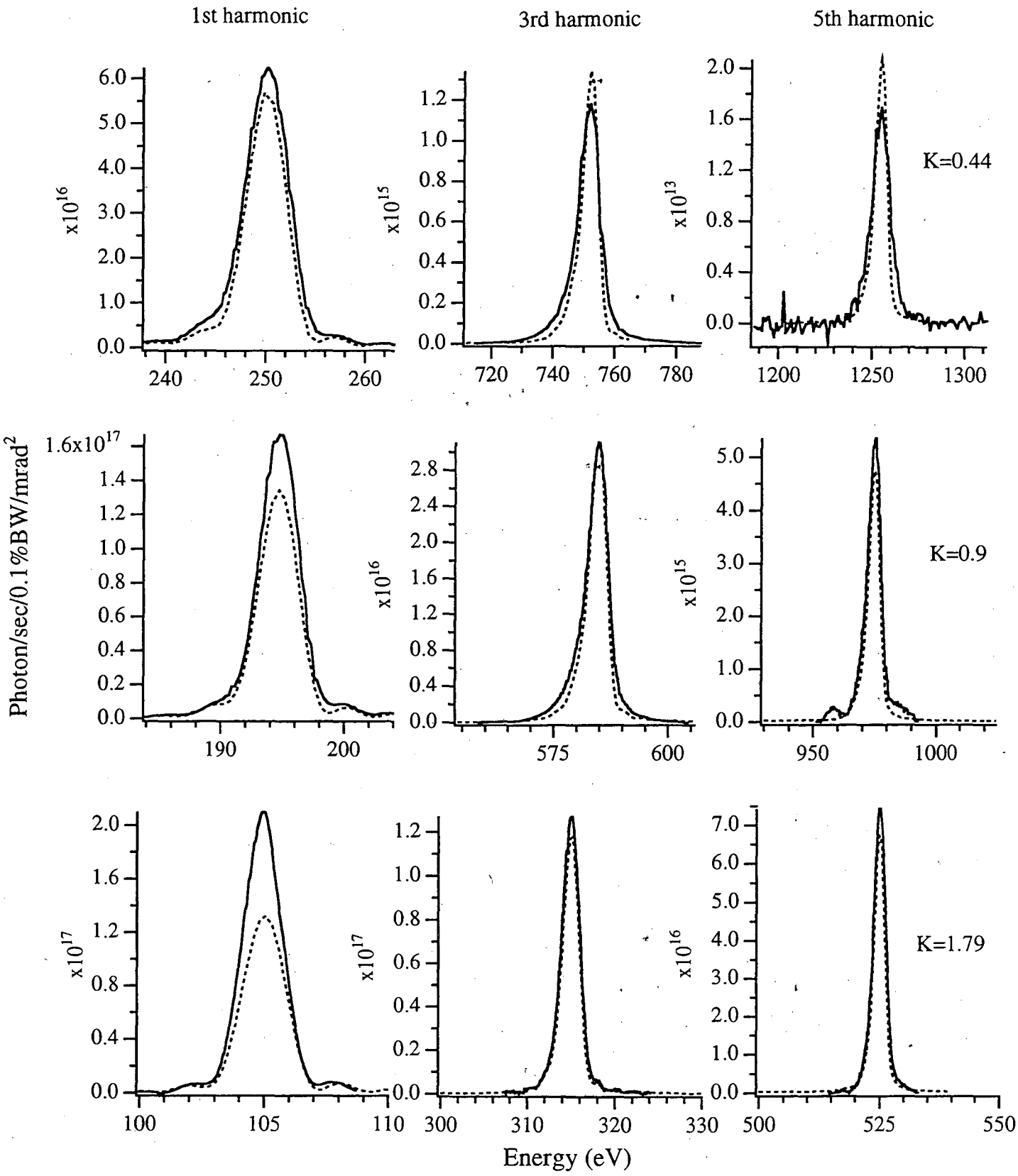

D.A. Mossessian
P.A. Deimann

Figure 4.

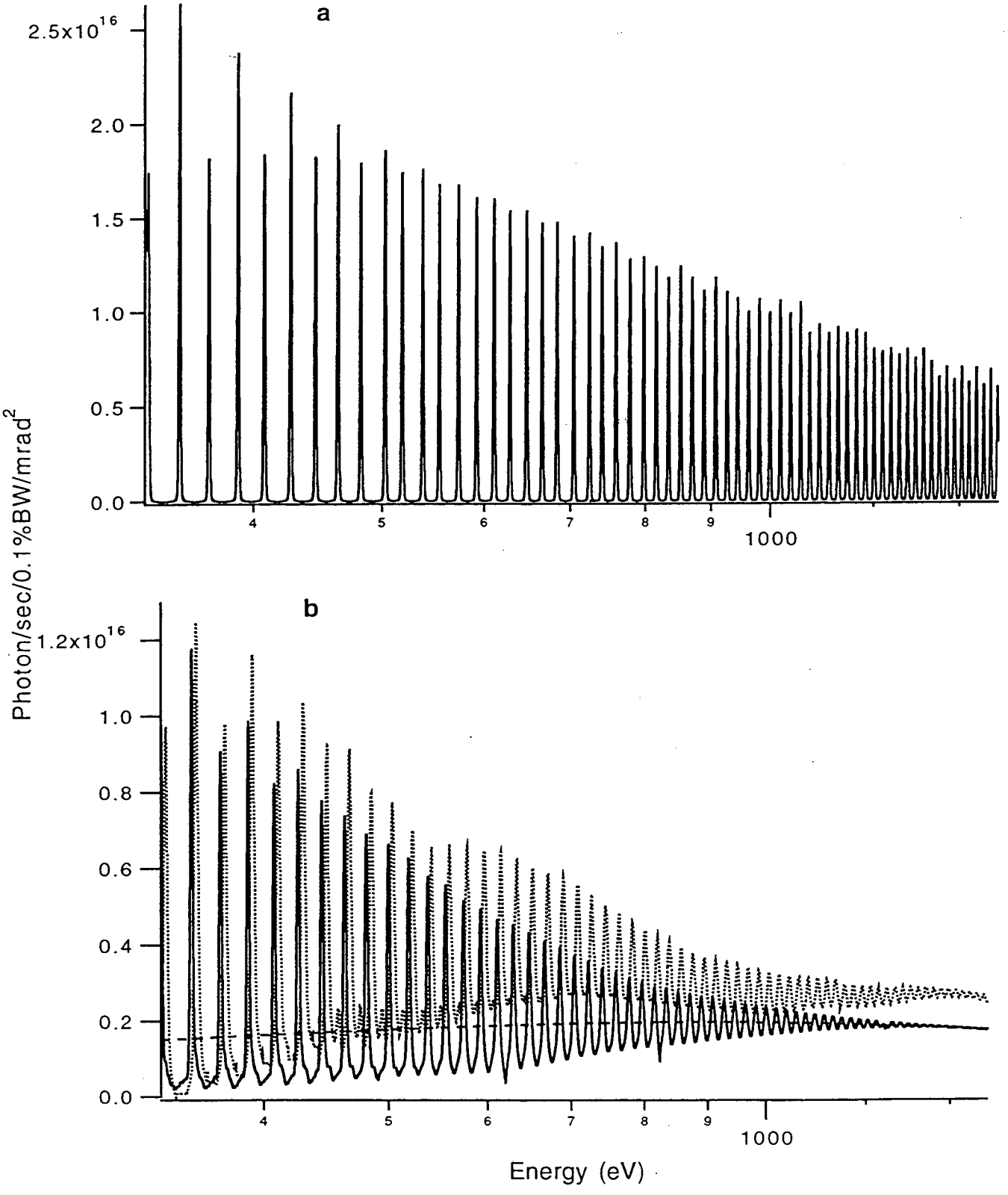

Figure 5

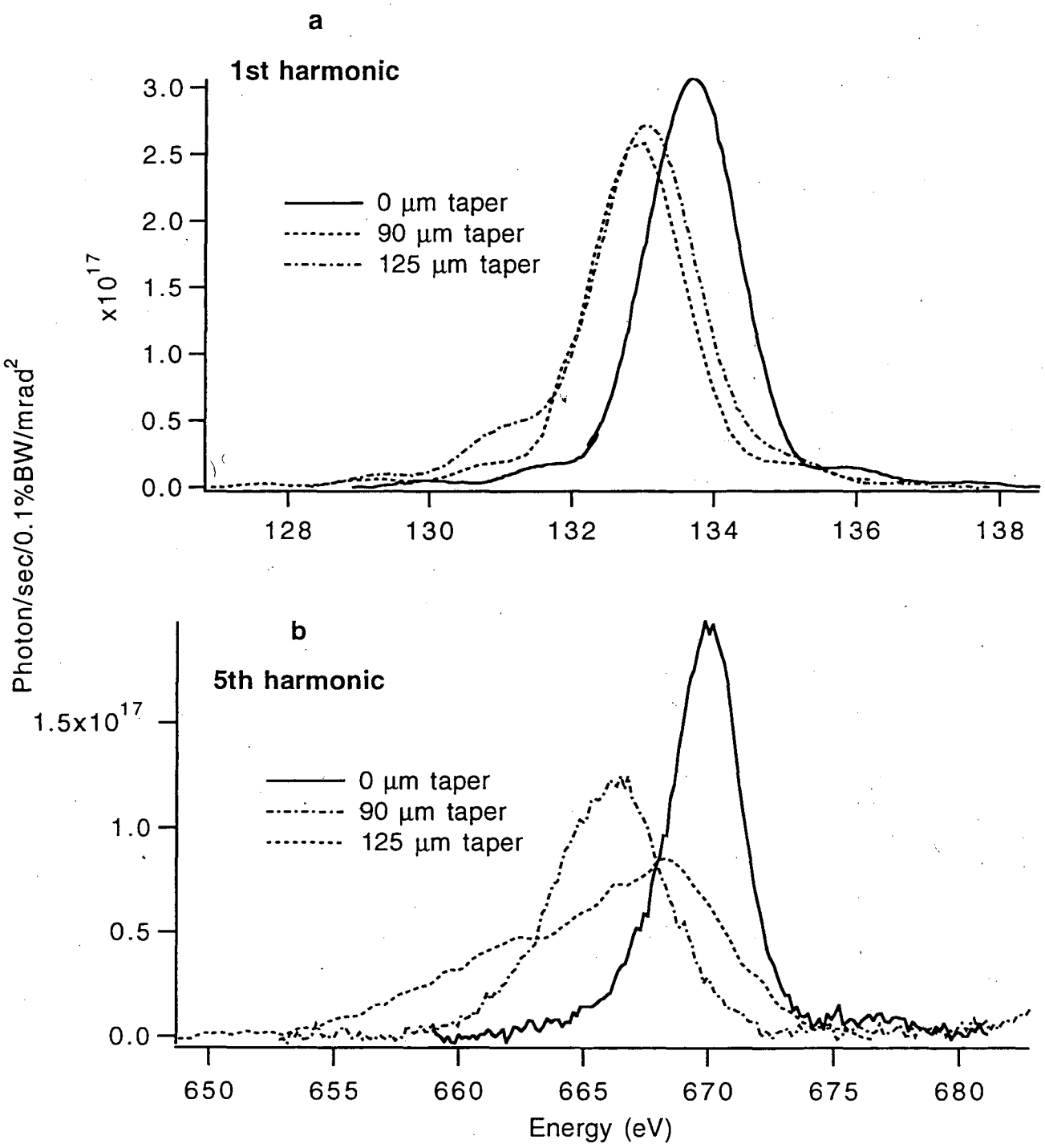
a
1st harmonic
3.0
2.5
2.0
1.5
1.0
0.5
0.0
x10^17
0 μm taper
90 μm taper
125 μm taper
128
130
132
134
136
138
Photon/sec/0.1%BW/mrad^2
b
5th harmonic
1.5x10^17
1.0
0.5
0.0
0 μm taper
90 μm taper
125 μm taper
650
655
660
665
670
675
680
Energy (eV)

D.A. Mossessian
P.L. Reimann

Figure 6

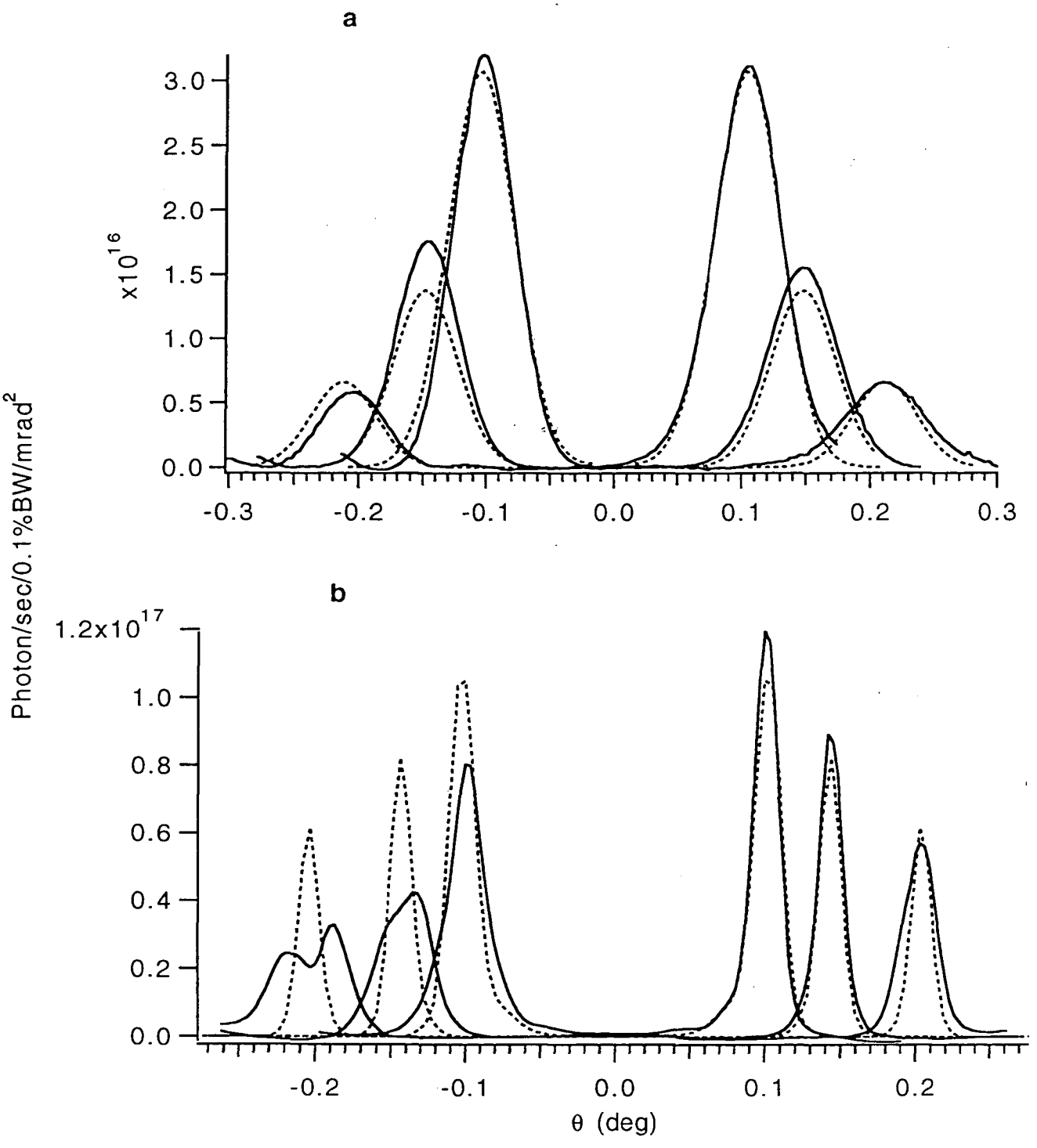

D.H. Mossessian P.H. Heimann

Figure 7

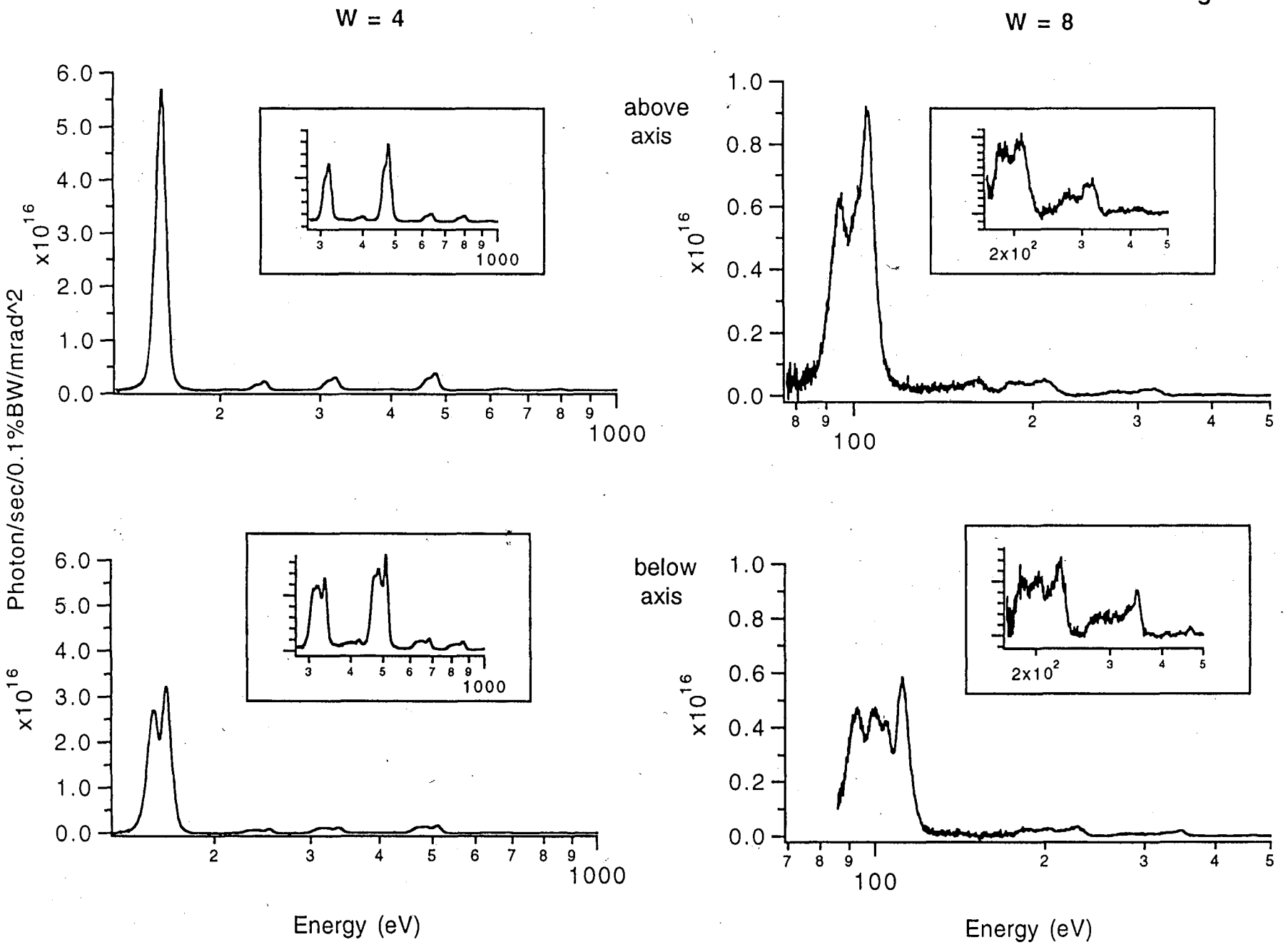

LAWRENCE BERKELEY LABORATORY
UNIVERSITY OF CALIFORNIA
TECHNICAL AND ELECTRONIC
INFORMATION DEPARTMENT
BERKELEY, CALIFORNIA 94720